



Published in final edited form as:

Nature. 2010 May 20; 465(7296): 359–362. doi:10.1038/nature09022.

Calcium-dependent protein kinase 1 is an essential regulator of exocytosis in *Toxoplasma*

Sebastian Lourido¹, Joel Shuman¹, Chao Zhang², Kevan M. Shokat², Raymond Hui³, and L. David Sibley¹

¹Department of Molecular Microbiology, Washington University School of Medicine, 660 S. Euclid Ave., St. Louis, MO 63110

²Howard Hughes Medical Institute, Department of Cellular and Molecular Pharmacology, UCSF, San Francisco, CA

³Structural Genomics Consortium, University Toronto, MaRS South Tower, Suite 732, 101 College St., Toronto Canada M5G 1L7

Abstract

Calcium-regulated exocytosis is a ubiquitous process in eukaryotes, whereby secretory vesicles fuse with the plasma membrane and release their contents in response to an intracellular calcium surge¹. This process regulates diverse cellular functions like plasma membrane repair in plants and animals^{2,3}, discharge of defensive spikes in *Paramecium*⁴, and secretion of insulin from pancreatic cells, immune modulators from lymphocytes, and chemical transmitters from neurons⁵. In animal cells, serine/threonine kinases including PKA, PKC and CaM-kinases have been implicated in calcium-signal transduction leading to regulated secretion^{1,6,7}. Although plants and protozoa also regulate secretion via intracellular calcium, the means by which these signals are relayed have not been elucidated. Here we demonstrate that the *Toxoplasma gondii* calcium-dependent protein kinase 1 (TgCDPK1) is an essential regulator of calcium-dependent exocytosis in this opportunistic human pathogen. Conditional suppression of TgCDPK1 revealed that it controls calcium-dependent secretion of specialized organelles called micronemes, resulting in a block of essential phenotypes including parasite motility, host-cell invasion, and egress. This phenotype was recapitulated using a chemical biology approach, wherein pyrazolopyrimidine-derived compounds specifically inhibited TgCDPK1 and disrupted the parasite life cycle at stages dependent on microneme secretion. Inhibition was specific to TgCDPK1, since expression of a resistant kinase mutant reversed sensitivity to the inhibitor. TgCDPK1 is conserved among apicomplexans and belongs to a family of kinases shared with plants and ciliates⁸, suggesting that related CDPKs may play a role in calcium-regulated secretion in other organisms. Since this

Users may view, print, copy, download and text and data- mine the content in such documents, for the purposes of academic research, subject always to the full Conditions of use: http://www.nature.com/authors/editorial_policies/license.html#terms

Author Contributions S.L. designed and performed the majority of experiments, analyzed the data, generated the figures, and wrote the manuscript. J.S. performed the video microscopy measurements of motility and analyzed the data. R.H. provided key insight into the regulation of CDPKs by calcium. C.Z. and K.M.S. provided inhibitors and insight into the strategy for chemical biology experiments. L.D.S. supervised the project, assisted with experimental design and analyses, and contributed to writing the manuscript.

The authors have no competing interests.

kinase family is absent from mammalian hosts, it represents a validated target that may be exploitable for chemotherapy against *T. gondii* and related apicomplexans.

The apicomplexan parasite *T. gondii* has been used as a model for the secretion of numerous proteins from specialized organelles, called micronemes, in response to increased intracellular calcium⁹. Microneme secretion can be blocked by broad-spectrum serine/threonine kinase inhibitors, and this is not circumvented by addition of calcium ionophores, suggesting kinases mediate the transduction of the calcium signal¹⁰. Calcium-dependent protein kinases (CDPKs), have been identified in plants, ciliates, and apicomplexans, but are absent in fungi and animals¹¹. CDPKs can respond to calcium when their calmodulin-like domain binds calcium and releases the kinase domain from an inactive conformation¹¹. Recent structural studies illustrate a novel mechanism of CDPK activation that results from a large-scale intramolecular rearrangement¹². Apicomplexans contain a diverse family of CDPKs, some of which have canonical domain structures, while others are more diverse⁸. In *Plasmodium*, the causative agent of malaria, gene knockouts of several individual CDPKs have revealed important roles at specific developmental stages⁸. For example, disruption of CDPK4 in *Plasmodium berghei* asexual stages leads to differentiation defects in male gametocytes¹³; a block which currently precludes analysis of its role in other motile stages such as sporozoites. The orthologue of this kinase is called TgCDPK1 in *T. gondii* and a previous study suggested the ability of KT5926, a pan-specific S/T kinase inhibitor related to staurosporine, to block cell attachment may result from inhibition of this target¹⁴. Although KT5926 inhibits TgCDPK1 activity *in vitro*¹⁴, it is unlikely to provide specific inhibition in the parasite, which harbors 11 distinct CDPKs⁸ that control largely unexplored cellular pathways.

To precisely define the role of TgCDPK1 in the parasite life-cycle, we generated a conditional knockout (cKO) using the tetracycline trans-activator system, previously developed for the study of essential genes in *Toxoplasma*¹⁵. We first engineered a strain expressing a HA9-tagged allele of TgCDPK1 driven by a modified TetOSAG1 promoter, permitting repression of the transgene during growth in anhydrotetracycline (ATc; Fig. 1a). The endogenous *TgCDPK1* gene was then replaced by double homologous recombination, generating the cKO as confirmed by PCR analysis (Fig 1a,b). Different alleles, expressed under the *SAG1* constitutive promoter, were subsequently introduced into the cKO to test for complementation. Growth of the cKO in ATc resulted in nearly undetectable levels of the HA9-tagged regulatable protein, while the c-Myc-tagged constitutive proteins were stably expressed in the complemented strains (Fig. 1, c and d). As a first assessment of the essentiality of TgCDPK1, we tested the ability of parasites to form plaques on host cell monolayers. Both WT and cKO lines grew normally in the absence of ATc, while the presence of ATc led to a complete block in plaque formation in only the cKO (Fig. 1e). The phenotype was fully rescued when complemented with the wild type allele (cKO/WT; Fig. 1e) but not by a mutant allele where the catalytic aspartate was mutated to an alanine (cKO/D¹⁷⁴A; Fig. 1e), indicating that TgCDPK1 function requires an active kinase.

Motility in apicomplexan parasites depends on a unique system whereby adhesins contained in the micronemes are released onto the apical end of the parasite and translocated to the

posterior of the cell, thus propelling the parasite forward¹⁶. Down regulation of TgCDPK1 by addition of ATc during intracellular growth did not affect parasite replication, yet parasites harvested from such cultures were significantly impaired in all forms of gliding motility (Fig. 2a). Those few cKO parasites that were able to glide, presumably due to leaky suppression, exhibited wild type speeds of motility, indicating that the motor complex itself was unaffected (Supplementary Fig.1). Gliding motility is normally prerequisite for cell invasion¹⁶ and consistent with this, the cKO experienced greater than 90% reduction in invasion when grown in the presence of ATc (Fig. 2b). Just as with plaque formation, invasion could be rescued by expression of the constitutive *WT* allele, but not the kinase-dead allele (Fig. 2b). Interestingly, suppression of TgCDPK1 also resulted in a strong reduction in host cell attachment (Fig. 2b), suggesting it affects an early step in invasion.

Egress from host cells depends on many of the same cellular pathways required for invasion, and this pathway may naturally be triggered by accumulation of the plant-like hormone abscisic acid¹⁷. The cKO parasites grown in the absence of ATc, behaved like WT and rapidly egressed from host cells in response to calcium ionophore treatment, an artificial but potent trigger of egress¹⁸ (Fig. 2c, Supplementary Movie 1, Supplementary Table 1). In contrast, virtually all cKO parasites grown in the presence of ATc did not respond to ionophore, remaining immotile within the vacuole (Fig. 2c, Supplementary Movie 2, Supplementary Table 1). Together these experiments indicate that TgCDPK1 is essential for the transduction of the calcium signals regulating gliding motility, invasion, and egress.

All of the above TgCDPK1-dependent phenotypes share a requirement for adhesins stored in micronemes, which undergo calcium-regulated exocytosis, in contrast to other secretory compartments such as dense granules, which are constitutively released⁹. Interestingly, TgCDPK1 shares a similar expression pattern to known microneme proteins, as detected by microarray analysis of synchronized parasites (95% C.I.; M. Behnke and M. White unpublished data). Together, these data suggested that TgCDPK1 might regulate microneme secretion, releasing, among other proteins, the well-studied adhesin MIC2⁹. Following secretion onto the cell surface, MIC2 is translocated to the cell posterior and shed from the parasite surface by proteolysis, allowing for the detection of secreted MIC2 in the supernatant¹⁹. As expected, MIC2 was detected in the supernatant of WT parasites stimulated with ethanol, which is another potent secretagogue that is thought to act through phospholipase C²⁰ (Fig. 3a). In contrast, the amount of MIC2 secreted by the cKO parasites grown in the presence of ATc was nearly undetectable, demonstrating a severe defect in calcium-regulated exocytosis (Fig. 3a). Secretion of MIC2 was restored to wild type levels by the constitutive *WT* allele, but not by the kinase dead allele (Fig. 3a). Growth of the cKO in ATc did not affect dense granule release (Fig. 3a), demonstrating that TgCDPK1 specifically regulates calcium-dependent exocytosis from micronemes, and not other secretory pathways.

Microneme secretion also plays an important role in parasite egress releasing the perforin-like protein TgPLP1 that aids in permeabilization of the parasitophorous vacuole membrane (PVM)²¹. To assess the role of TgCDPK1 in controlling microneme secretion during egress, we generated WT and cKO lines expressing a constitutively secreted form of DsRed, allowing for the visualization of PVM integrity by live video microscopy. To avoid

premature rupture of the vacuole, parasites were treated with cytochalasin D to immobilize them and allow selective monitoring of the kinetics of PVM rupture by leakage of DsRed. As previously reported²¹, WT parasites rapidly permeabilized the PVM upon calcium-ionophore treatment, releasing DsRed into the host-cell cytoplasm (Fig. 3b, Supplementary Movie 3). All WT vacuoles showed rapid PVM permeabilization (average 1.7 ± 0.5 min, s.d.), whereas approximately 30% of cKO parasites grown in the presence of ATc failed to rupture the PVM (Fig. 3c, Supplementary Movie 4; data not shown). Analysis of those cKO parasite vacuoles that did rupture, showed a significant delay in the timing and rate of DsRed release when compared to WT vacuoles (Fig. 3c, d). Collectively, these results demonstrate a requirement for TgCDPK1 in controlling the release of microneme contents including TgPLP1 during egress. Moreover, the inability of calcium-ionophore to circumvent the requirement for TgCDPK1, places this kinase as the critical transducer downstream of the calcium signal regulating microneme exocytosis.

Having established the crucial role of TgCDPK1, we took advantage of the atypical nucleotide-binding pocket of TgCDPK1¹² to develop a chemical biology approach to further evaluate the essential nature of this kinase. It has been previously reported that the amino acid residue at the “gatekeeper” position within the nucleotide binding pocket radically affects inhibition by pyrazolopyrimidine (PP1) derivatives, which have limited activity against most S/T protein kinases²². Insensitivity is conferred by bulky gatekeeper residues in nearly all kinases of both animal and parasite cells; however, kinases can be rendered fully sensitive by mutation to a small gatekeeper²² (Supplementary Table 2). Fortuitously, TgCDPK1 displays a glycine at this position, which is unique among canonical CDPKs (Fig. 4a) and all other protein kinases in *T. gondii* (L. Peixoto and D. Roos, unpublished data). This finding predicted that wild type TgCDPK1 would be naturally sensitive to PP1-based inhibitors and, consistent with this a pilot screen of selected derivatives inhibited parasite lytic growth *in vitro* (Supplementary Fig. 2). Furthermore, purified TgCDPK1 enzyme was extremely sensitive to the compound 3-MP-PP1 (Fig. 4b), while mutation of the glycine gatekeeper to methionine shifted the sensitivity by more than 4 logs (Supplementary Table 2). Complementation of the TgCDPK1 cKO with either wild type or gatekeeper-mutant kinase alleles (cKO/WT and cKO/*G*¹²⁸*M*, respectively) restored plaque formation, demonstrating that the mutation had no major deleterious effect (Supplementary Fig. 3). When treated with PP1 analogs, both WT and cKO/WT parasites were strongly inhibited in host cell attachment and invasion (Fig. 4c), consistent with a recent report that appeared online during the revision of the present work²³. In contrast to this recent report, which failed to provide quantitative analysis of secretion²³, we observed that microneme secretion by extracellular parasites and ionophore-induced egress (Supplementary Fig. 4) were also strongly inhibited by PP1 analogs (Fig. 4d). The reversal of these phenotypes in the *G*¹²⁸*M* mutant confirms that the primary *in vivo* target of PP1 derivatives is TgCDPK1. Consistent with these effects, 3-MB-PP1 and the related compound 3-BrB-PP1, blocked the ability of the parasite to lyse host cell monolayers (Fig. 4e,f), demonstrating the essential role of TgCDPK1 during *in vitro* infection. Chemical genetic studies indicate that TgCDPK1 acts independently of the previously characterized cGMP-dependent kinase (PKG), the primary target of trisubstituted pyrole and imidazopyridine kinase inhibitors that also block microneme secretion in *T. gondii*^{24,25}. Correspondingly, PKG is predicted to be insensitive

to PP1 derivatives (Fig. 4a)²². Collectively these findings indicate that both kinases are essential for efficient microneme secretion, possibly reflecting a hierarchical control of this important cellular pathway.

Our findings demonstrate that TgCDPK1 acts downstream of the second messenger calcium to regulate exocytosis in *T. gondii*, thus controlling several essential biological steps in the life cycle. Nearly all mammalian protein kinases normally show very low sensitivity to PP1 derivatives²², making them potential lead compounds for development of specific anti-parasitic drugs. In addition, CDPKs may regulate calcium-dependent exocytosis in related parasites or other organisms like ciliates and plants, representing an evolutionary precedent to calmodulin-dependent kinases that regulate exocytosis in animals.

METHODS SUMMARY

Growth of host cells and parasite strains

T. gondii tachyzoites were maintained by growth in human foreskin fibroblasts, as previously described²⁶. Complemented strains were grown in 3 μ M pyrimethamine (Sigma) and ATc (Clontech) was added (1.5 μ g/ml) for 72h unless otherwise indicated. For inhibitor studies, parasites were incubated in the indicated concentration of 3-MB-PP1, 3-BrB-PP1, or DMSO control, for 20 min at RT, prior to use in assays.

Cellular assays

Plaque formation and invasion assays were performed as previously described^{27,28}. Microneme secretion was assayed by monitoring the release of MIC2 into the culture medium following stimulation with 3%FBS and 2% ethanol, 15 min at 37°C, as previously described²⁰. Samples were resolved by SDS-PAGE, blotted and probed with mouse- α -MIC2 (mAb 6D10), and mouse- α -GRA1 (mAb Tg17-43) and quantified by phosphoimager analysis. Egress and PVM permeabilization were monitored by video microscopy following stimulation with 8 μ M calcium-ionophore A23187 (Calbiochem). When noted, parasites were pre-treated for 10 min with 2 μ M Cytochalasin D (Calbiochem) to block motility. The extent and rate of egress, as well as degree of vacuole permeability was quantified using Openlab v. 4.1 (Improvision) as described in the supplementary materials. Host cell lysis was assayed by staining monolayers with crystal violet, 3 days after infection at an MOI of 1.

METHODS

Growth of host cells and parasite strains

T. gondii tachyzoites were maintained by growth in monolayers of human foreskin fibroblasts (HFFs) cultured in Dulbecco's modified Eagle's medium containing 10% tetracycline-free fetal bovine serum (HyClone), 2mM glutamine, 10mM HEPES (pH 7.5), and 20 μ g/ml gentamicin. Chloramphenicol (20 μ g/ml; Sigma), phleomycin (5 μ g/ml; InvivoGen), ATc (1.5 μ g/ml; Clontech), and pyrimethamine (3 μ M; Sigma) were added to the media as indicated, and for the maintenance of merodiploid or complemented strains. When noted, parasites were treated with ATc for 72h.

Strain construction

The TgCDPK1 cKO was constructed using tetracycline transactivator system¹⁵, as previously described for TgALD1²⁶. Briefly, *TgCDPK1* (Genbank accession number AF333958) was cloned with a C-terminal HA9-tag into the pTetO7SAG1 vector (obtained from Dominique Soldati), downstream of the inducible promoter, and the *CAT* selectable marker driven by the *SAG1* promoter was introduced at a different site. The TATi-1 strain (obtained from Dominique Soldati), used as the wild type (WT) background in this study, was transfected with the regulatable construct, and stable merodiploids were selected with chloramphenicol²⁹, and cloned by limiting dilution. To generate the knockout construct the *Ble* selectable marker³⁰ was flanked with 1.5kb upstream of the *TgCDPK1* start codon and 1.5kb downstream of the stop codon, followed by a YFP expression cassette²⁶. The knockout construct was linearized and transfected into the merodiploid strain and stable pools were selected through two rounds of phleomycin selection³⁰. Sorting for YFP-negative parasites was used to enrich for successful knockouts and individual clones were isolated by limiting dilution. Knockout of the endogenous *TgCDPK1* gene was confirmed in clones by polymerase chain reaction, using primers against consecutive exons and the intervening intron, to distinguish between the endogenous and regulatable genes. Complementing plasmids were constructed by cloning *TgCDPK1* with a carboxyl-terminal c-Myc-tag, under the regulation of the *SAG1* promoter. The *DHFR* selectable marker conferring pyrimethamine resistance³¹ was cloned into the complementing vectors. For the inhibitor studies, *SAG1* was replaced with the 1.5kb region preceding the *TgCDPK1* start codon. Co-transfection with pDHFR-TS³¹ was used to generate stable clones. Mutations were generated by site directed mutagenesis. Complementing plasmids were transfected into the cKO, stable lines were selected with pyrimethamine, and clones were isolated by limiting dilution. To monitor PVM permeabilization, WT and cKO strains were transfected with p30-DsRed²¹ (obtained from Florence Dzierszinski) and pDHFR-TS for isolation of stable transgenic lines as described above.

Plaque assay

Plaque assays were performed as previously described²⁷. Confluent monolayers of human foreskin fibroblasts in 6-well plates were infected with 200 parasites per well in media with or without 1.5µg/ml ATc (Clontech). 24 h post infection additional media was added reduce the concentration of ATc to 1µg/ml. Monolayers were fixed 7 days post infection and stained with crystal violet. Experiments were repeated three times with triplicate wells / experiment.

Invasion assay

Parasites were harvested in invasion media (Dulbecco's modified Eagle's medium containing 20 mM HEPES, pH 7.5, supplemented with 3% FBS). 5×10^6 parasites in a 250µl volume were added to sub-confluent HFF monolayers in 24-well plates and allowed to invade for 20 min. Monolayers were then fixed and stained as previously described²⁸ to distinguish extracellular from total parasites. Three experimental replicates were performed for each strain in each of three separate experiments and parasite numbers per field were

normalized to host-cell nuclei. For the inhibitor studies, parasites were incubated in 5 μ M 3-MB-PP1 or vehicle-only control (DMSO), for 20 min at room temperature, prior to invasion.

Host-lysis assay

Parasites were harvested and incubated in the indicated inhibitor or DMSO concentrations for 20 min at room temperature, prior to incubation with confluent monolayers in 96-well plates at an MOI of 1. For experiments comparing complemented strains, parasites were grown in 1.5 μ g/ml ATc for 72 h prior to harvesting. Parasites were allowed to invade for 1 hour, monolayers were washed 3-5 times and fresh media containing 1 μ g/ml ATc was added. The infection was allowed to progress 3 days before fixing with 70% ethanol and staining with crystal violet. Host-cell lysis was determined by measuring absorbance at 570nm in an EL800 microplate reader (BioTek Instruments, Inc.).

Immunofluorescence microscopy

Intracellular parasites were stained as previously described²⁶. MIC2 staining within the micronemes required a 2 min permeabilization with cold 100% ethanol on ice. Staining was performed with rabbit- α -HA9 (Invitrogen) and mouse- α -MIC2 (mAb 6D10), followed by Alexa564-goat- α -rabbit IgG (Invitrogen), Cy5-goat- α -mouse IgG (Jackson) and Sytox green (Invitrogen) for the nuclear stain. Images were collected on a Zeiss LSM 510 confocal microscope.

Video microscopy and quantitation of gliding motility

Gliding and egress were analyzed by video microscopy as previously described³². For gliding, 75 images were taken with exposure times ranging from 50-100 milliseconds with 1 second between exposures. Images were collected and combined into composites using Openlab v. 4.1 (Improvision). ImageJ was used to analyze the images. The ParticleTracker plug-in was used to track cell motility and Cell Counter was used to quantify percent motility.

Ionophore-induced egress and PVM permeabilization

Egress and PVM permeabilization were monitored by video microscopy as described above. Where noted, parasites were pre-incubated for 10 min in media containing 2 μ M Cytochalasin D (Calbiochem) at 37°C. All dishes were allowed to equilibrate for 5 min on the heated stage, prior to the addition of 8 μ M calcium ionophore A23187 (Calbiochem). Vacuoles were imaged for up to 10 min after the addition of ionophore. To quantify vacuole permeabilization the fluorescence intensity within a 80 μ m² region of each vacuole was measured using Openlab. The values for each vacuole were normalized against the starting (100%) and ending (0%) values for that particular vacuole, and the derivative of the curve was used to find the maximal rate of fluorescence loss and the time when that rate occurred. For the inhibitor studies, parasites were pre-treated with 5 μ M 3-MB-PP1 or vehicle-only control (DMSO) for 20 min at 37°C, prior to the addition of ionophore.

MIC2 secretion assay

Microneme secretion was assayed as previously described²⁰ by monitoring the release of MIC2 into the culture medium. Secretion was stimulated by treatment with 3% FBS and 2% ethanol, 15 min at 37°C. Parasite lysis was monitored by the release of actin into the medium and remained undetectable in all experiments presented. GRA1 secretion was used as a control for constitutive secretion. Samples were resolved by SDS-PAGE, blotted and probed with mouse- α -MIC2 (mAb 6D10), rabbit- α -TgACT1, and mouse- α -GRA1 (mAb Tg17-43, kindly provided by Marie France Cesbron, Genoble, France). Quantitation was performed by densitometry using a FLA-5000 phosphoimager (Fuji Medical Systems). For the inhibitor studies, parasites were pre-treated with 5 μ M 3-MB-PP1 or vehicle-only control (DMSO) for 20 min at 37°C, prior to stimulation.

In vitro IC₅₀ determination

Full-length His-tagged TgCDPK1 was cloned into the pET-22b(+) vector (Novagen) and expressed in *Escherichia coli* BL21. Point mutations were generated using QuickChange site-directed mutagenesis (Stratagene). Proteins were induced with IPTG and purified using nickel-affinity chromatography. Activities of WT and G^{128M} TgCDPK1 were determined using the CycLex CaM Kinase II Assay Kit (MBL International Corporation) according to manufacturer's instructions. c-Src proteins were expressed and assayed in the presence of various concentrations of the inhibitors as previously described³³. IC₅₀ was determined by fitting dose response curve with the GraphPad Prism software.

Statistics

Experiments were repeated three or more times and statistical analyses conducted in Excel using the Student's t test (unpaired, equal variance, two-tailed test) for comparisons with data that fit a normal distribution or the Mann-Whitney test for non-parametric comparisons.

Supplementary Material

Refer to Web version on PubMed Central for supplementary material.

Acknowledgements

We thank Gary Ward, Silvia Moreno, and Vern Carruthers for discussions, Florence Dzierszinski for the DsRed plasmid, Dominique Soldati for the Tet-repression system, and Keliang Tang for technical assistance. This work was supported by a predoctoral fellowship from the American Heart Association (S.L.) and a grant from the NIH (L.D.S.).

REFERENCES

1. Barclay JW, Morgan A, Burgoyne RD. Calcium-dependent regulation of exocytosis. *Cell Calcium*. 2005; 38:343–353. [PubMed: 16099500]
2. Schapire AL, Valpuesta V, Botella MA. Plasma membrane repair in plants. *Trends Plant Sci*. 2009; 14:645–652. [PubMed: 19819752]
3. Bansal D, Campbell KP. Dysferlin and the plasma membrane repair in muscular dystrophy. *Trends Cell Biol*. 2004; 14:206–213. [PubMed: 15066638]
4. Vayssie L, Skouri F, Sperling L, Cohen J. Molecular genetics of regulated secretion in paramecium. *Biochimie*. 2000; 82:269–288. [PubMed: 10865117]

5. Chieregatti E, Meldolesi J. Regulated exocytosis: new organelles for non-secretory purposes. *Nat. Rev. Mol. Cell Biol.* 2005; 6:181–187. [PubMed: 15688003]
6. Choi WS, Chahdi A, Kim YM, Fraundorfer PF, Beaven MA. Regulation of phospholipase D and secretion in mast cells by protein kinase A and other protein kinases. *Ann. N. Y. Acad. Sci.* 2002; 968:198–212. [PubMed: 12119277]
7. Easom RA. CaM kinase II: a protein kinase with extraordinary talents germane to insulin exocytosis. *Diabetes.* 1999; 48:675–684. [PubMed: 10102681]
8. Billker O, Lourido S, Sibley LD. Calcium-dependent signaling and kinases in apicomplexan parasites. *Cell Host Microbe.* 2009; 5:612–622. [PubMed: 19527888]
9. Carruthers VB, Sibley LD. Mobilization of intracellular calcium stimulates microneme discharge in *Toxoplasma gondii*. *Mol. Microbiol.* 1999; 31:421–428. [PubMed: 10027960]
10. Carruthers VB, Giddings OK, Sibley LD. Secretion of micronemal proteins is associated with *Toxoplasma* invasion of host cells. *Cell Microbiol.* 1999; 1:225–236. [PubMed: 11207555]
11. Harper JF, Harmon AC. Plants, symbiosis and parasites: a calcium signalling connection. *Nat. Rev. Molec. Cell Biol.* 2005; 6:555–566. [PubMed: 16072038]
12. Wernimont A, et al. Structural analysis of calcium-dependent protein kinases reveal mechanism of activation by calcium. *Nat. Struc. Molec. Biol.* 2010 in press.
13. Billker O, et al. Calcium and a calcium-dependent protein kinase regulate gamete formation and mosquito transmission in a malaria parasite. *Cell.* 2004; 117:503–514. [PubMed: 15137943]
14. Kieschnick H, Wakefield T, Narducci CA, Beckers C. *Toxoplasma gondii* attachment to host cells is regulated by a calmodulin-like domain protein kinase. *J. Biol. Chem.* 2001; 276:12369–12377. [PubMed: 11154702]
15. Meissner M, Schluter D, Soldati D. Role of *Toxoplasma gondii* myosin A in powering parasite gliding and host cell invasion. *Science.* 2002; 298:837–840. [PubMed: 12399593]
16. Sibley LD. Invasion strategies of intracellular parasites. *Science.* 2004; 304:248–253. [PubMed: 15073368]
17. Nagamune K, et al. Abscisic acid controls calcium-dependent egress and development in *Toxoplasma gondii*. *Nature.* 2008; 451:207–211. [PubMed: 18185591]
18. Endo T, Sethi KK, Piekarski G. *Toxoplasma gondii*: calcium ionophore A23187-mediated exit of trophozoites from infected murine macrophages. *Exp. Parasitol.* 1982; 53:179–188. [PubMed: 6800836]
19. Carruthers VB, Sherman GD, Sibley LD. The *Toxoplasma* adhesive protein MIC2 is proteolytically processed at multiple sites by two parasite-derived proteases. *J. Biol. Chem.* 2000; 275:14346–14353. [PubMed: 10799515]
20. Carruthers VB, Moreno SNJ, Sibley LD. Ethanol and acetaldehyde elevate intracellular $[Ca^{2+}]$ calcium and stimulate microneme discharge in *Toxoplasma gondii*. *Biochem. J.* 1999; 342:379–386. [PubMed: 10455025]
21. Kafsack BF, et al. Rapid membrane disruption by a perforin-like protein facilitates parasite exit from host cells. *Science.* 2009; 323:530–533. [PubMed: 19095897]
22. Bishop AC, et al. A chemical switch for inhibitor-sensitive alleles of any protein kinase. *Nature.* 2000; 407:395–401. [PubMed: 11014197]
23. Sugi T, et al. Use of the kinase inhibitor analog 1NM-PP1 reveals a role for *Toxoplasma gondii* CDPK1 in the invasion step. *Eukaryot Cell.* 2010 in press.
24. Gurnett AM, et al. Purification and molecular characterization of cGMP-dependent protein kinase from Apicomplexan parasites. A novel chemotherapeutic target. *J. Biol. Chem.* 2002; 277:15913–15922. [PubMed: 11834729]
25. Wiersma HI, et al. A role for coccidian cGMP-dependent protein kinase in motility and invasion. *Intl. J. Parasit.* 2004; 34:369–380.
26. Starnes GL, Coincon M, Sygusch J, Sibley LD. Aldolase is essential for energy production and bridging adhesin-actin cytoskeletal interactions during parasite invasion of host cells. *Cell Host Microbe.* 2009; 5:353–364. [PubMed: 19380114]
27. Roos DS, Donald RGK, Morrissette NS, Moulton AL. Molecular tools for genetic dissection of the protozoan parasite *Toxoplasma gondii*. *Methods Cell Biol.* 1994; 45:28–61.

28. Huynh MH, et al. Rapid invasion of host cells by *Toxoplasma* requires secretion of the MIC2-M2AP adhesive protein complex. *EMBO J.* 2003; 22:2082–2090. [PubMed: 12727875]
29. Kim K, Soldati D, Boothroyd JC. Gene replacement in *Toxoplasma gondii* with chloramphenicol acetyltransferase as selectable marker. *Science.* 1993; 262:911–914. [PubMed: 8235614]
30. Messina M, Niesman IR, Mercier C, Sibley LD. Stable DNA transformation of *Toxoplasma gondii* using phleomycin selection. *Gene.* 1995; 165:213–217. [PubMed: 8522178]
31. Donald RGK, Roos DS. Stable molecular transformation of *Toxoplasma gondii*: A selectable dihydrofolate reductase-thymidylate synthase marker based on drug resistance mutations in malaria. *Proc. Nat. Acad. Sci. (USA).* 1993; 90:11703–11707. [PubMed: 8265612]
32. Håkansson S, Morisaki H, Heuser JE, Sibley LD. Time-lapse video microscopy of gliding motility in *Toxoplasma gondii* reveals a novel, biphasic mechanism of cell locomotion. *Mol. Biol. Cell.* 1999; 10:3539–3547. [PubMed: 10564254]
33. Blair JA, et al. Structure-guided development of affinity probes for tyrosine kinases using chemical genetics. *Nat Chem Biol.* 2007; 3:229–238. [PubMed: 17334377]

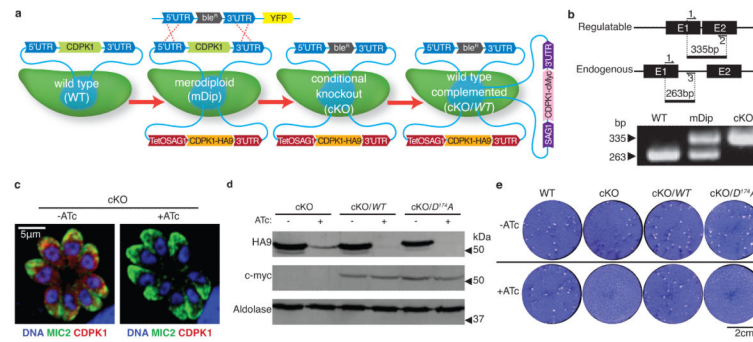


Figure 1. TgCDPK1 is essential for the lytic cycle

a, Regulatable, HA9-tagged TgCDPK1 was added to wild-type (WT) to create a merodiploid (mDip). Endogenous TgCDPK1 was replaced with phleomycin resistance (*ble^R*) to generate the cKO. Complementation with c-Myc tagged mutant alleles (denoted by cKO/“*allele*”). **b**, Multiplexed PCR analysis of TgCDPK1. **c**, Immunofluorescence analysis of the cKO +/-ATc; endogenous MIC2 (green), HA9-tag (red) and DNA (blue). **d**, Immunoblot of HA9-tagged regulatable and c-Myc-tagged constitutive TgCDPK1 in cKO and complemented strains +/- ATc. Aldolase, loading control. **e**, Plaque formation on fibroblast monolayers, +/- ATc for 7 days.

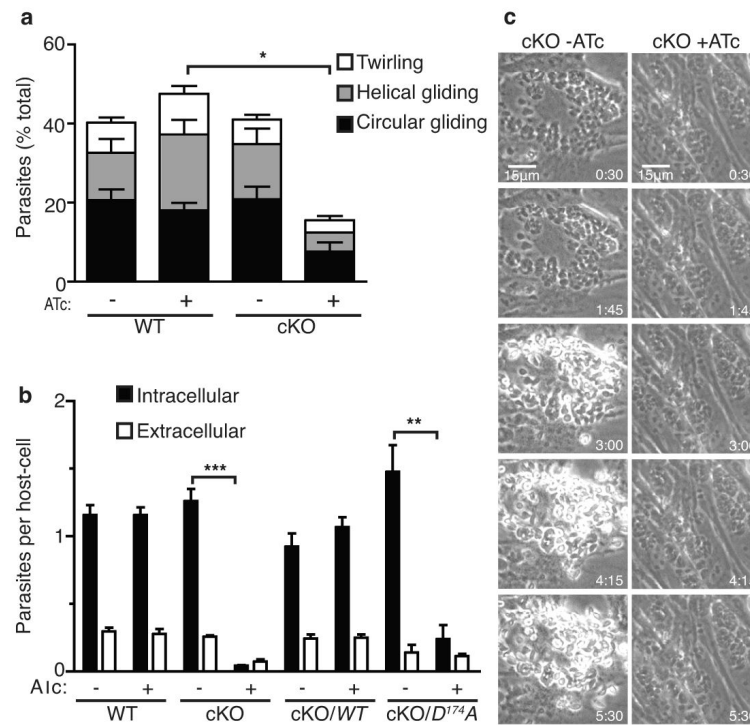


Figure 2. TgCDPK1 is required for phenotypes associated with microneme secretion

a, Types of gliding motility as quantified by video microscopy. Student's *t* test; * $P < 0.05$, mean \pm s.e.m., $N = 4$ experiments. **b**, Invasion of fibroblasts by WT, cKO and complemented strains. Extracellular and intracellular parasites were differentially stained and enumerated as described in supplementary materials. Student's *t* test; *** $P < 0.0005$, ** $P < 0.005$, mean \pm s.e.m., $N = 3$ experiments. **c**, Ionophore-induced egress of the cKO +/- ATc. Time stamp (min:sec) after calcium ionophore addition. See supplementary online videos.

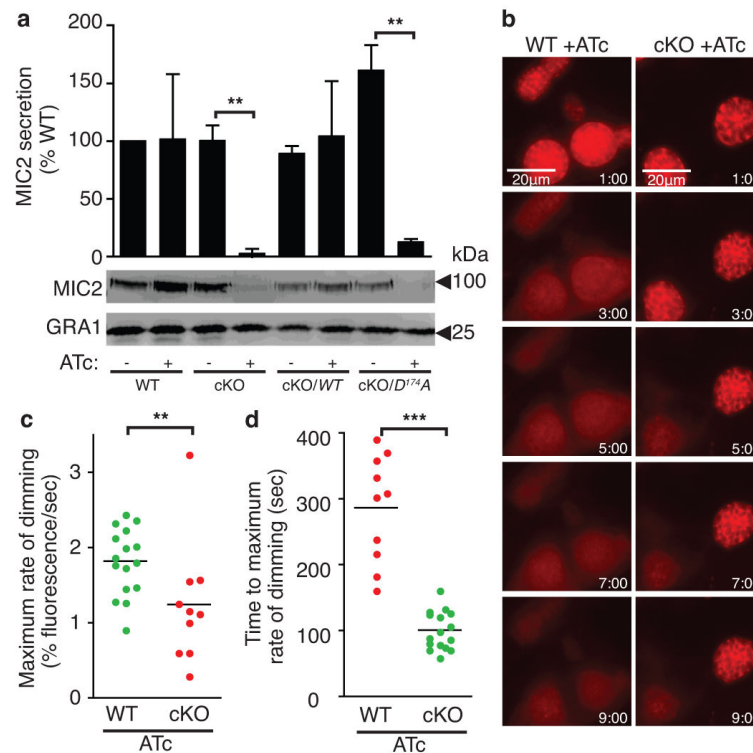


Figure 3. Calcium-dependent microneme secretion requires TgCDPK1

a, Western blot analysis of microneme protein MIC2 secretion following induction by ethanol for 15 min. GRA1 shows constitutive secretion of dense granules. Student's *t* test; $**P < 0.005$, mean \pm s.e.m., $N = 3$ experiments. **b**, Ionophore-induced permeabilization detected by vacuolar DsRed leakage monitored by fluorescence video-microscopy of strains 90h + ATc. Time stamp (min:sec) after calcium ionophore addition. CytochalasinD added to prevent egress. **c-d**, Quantification of maximal rate and timing of fluorescence loss from rupturing vacuoles. Mann-Whitney test; $***P < 0.0005$, $**P < 0.005$, mean, $N = 3$ experiments.

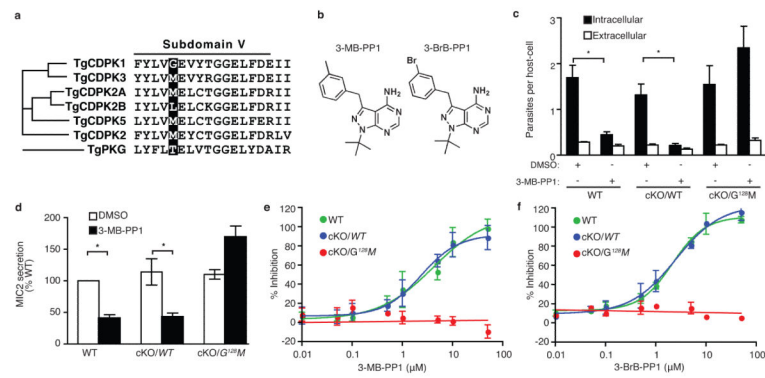


Figure 4. PP1 derivatives specifically inhibit TgCDPK1 and block micronem-mediated functions
a, Alignment of the kinase sub-domain V highlighting the gatekeeper residue. **b**, Structures of 3-MB-PP1 and 3-BrB-PP1. **c**, Effect of 5 μ M 3-MB-PP1 on host cell invasion. Student's *t* test; **P* < 0.05, mean \pm s.e.m., *N* = 3 experiments. **d**, Effect of 5 μ M 3-MB-PP1 on MIC2 secretion. Student's *t* test; **P* < 0.05, mean \pm s.e.m., *N* = 3 experiments. **e-f**, Effect of PP1 derivatives on host lysis by *T. gondii* +/- 3-MB-PP1 (**e**) and 3-Br-PP1 (**f**). Mean \pm s.e.m., *N* = 3 experiments.